Suitability of Commercial V2G CHAdeMO Chargers for Grid Services

Zecchino, Antonio; Thingvad, Andreas; Andersen, Peter Bach; Marinelli, Mattia

Published in:
Proceedings of EVS 31 & EVTeC 2018.

Publication date:
2018

Document Version
Peer reviewed version

Suitability of Commercial V2G CHAdeMO Chargers for Grid Services

V2G hardware tests with local and remote control setup: assessing the performance for quality grid services

Antonio Zecchino, Andreas Thingvad, Peter Bach Andersen, Mattia Marinelli

Center for Electric Power and Energy, Department of Electrical Engineering, Technical University of Denmark

Frederiksborgvej 399, Building 776, 4000 Roskilde, Denmark – e-mail: {antozec, athing, pba, matm}@elektro.dtu.dk

Presented at EVS 31 & EVTeC 2018, Kobe, Japan, October 1 - 3, 2018

ABSTRACT: Aggregation and control of electric vehicles (EVs) via vehicle-to-grid (V2G) technologies is seen as a valid option for providing ancillary power system services. This work presents results from V2G-ready equipment tests. The technical capabilities of an EV connected to a commercial V2G charger are investigated when controlled either locally or remotely. The charger is characterized in terms of efficiency characteristics, activation time, response granularity, ramping-up/down time, accuracy and precision. Results show the performance for different operating conditions, highlighting the importance of a good calibration and knowledge of the employed hardware when providing standard-compliant grid regulation services via V2G technology.

KEY WORDS: CHAdeMO, commercial EV chargers, electric vehicles, vehicle-to-grid

1. INTRODUCTION

Vehicle grid integration (VGI) research aims to support a seamless electrification of the transportation sector, proactively dealing with both challenges and opportunities which may arise. The term grid integrated vehicle (GIV) describes an electric vehicle (EV) purposely designed to limit its self-induced adverse effects in the power system, while also supporting the system by being able to provide a number of power and energy services. Such services may be aimed at achiving energy autonomy, supporting the local grid infrastructure or providing regional power and energy balancing [1], [2].

One class of system services EVs may provide is frequency containment reserves (FCR), which is required in the Nordic synchronous region. In order to provide such service, the EV charging or discharging would be controlled to support the system frequency. This service is interesting for two reasons. Firstly, the service is enumerated based on the available power [kW], not on the actual energy exchanged with the grid. Since the EV battery is an exhaustable resource in terms of energy but is capable of providing high instantaneous power, this represents a good technical match. Secondly, some markets already allow EV aggregators to participate in FCR provision. However, FCR is also one of the most technically demanding services with high requirements to a fast and reliable response and where access to vehcile-to-grid (V2G) strengthens the vehicles ability to provide the service considerably [3], [4].

Bidirectional V2G is presently only accessible through DC chargers using the CHAdeMO protocol. While DC chargers typically are associated with public fast-charging stations, reduction in size and price may ultimately allow for domestic use as well. A number of contemperary EV integration projects focused on V2G explore the use of early V2G-enabled DC chargers [5]–[8]. These chargers represent a key technology, enabling V2G across a broad number of EV models. It then becomes important to investigate the performance of these chargers on parameters specific to the provision of V2G based services – going beyond traditional one-way charging. This is the focus of this work, investigating the technical capabilities of V2G equipment when controlled either locally or remotely. This study presents an operational characterization of a commercial ±10 kW V2G DC charger [9] aimed at efficiency and active power control. Such characterization describes the extend to which DC chargers may be used to critical and demanding smart grid services such as FCR.

2. THE NEED FOR HARDWARE PERFORMANCE ASSESSMENT WHEN CONTROLLING EVS

In order to correctly procure the amount of reserve needed for ancillary services, it is necessary to define the most important attributes characteristing the unit response. The flexibility product can be defined as *the power adjustment sustained from a particular moment for a certain duration at a specific location* [10]. Given the nature of the service provided, the flexibility product can be either active or reactive power adjustment. However, as in this work reactive power exchange was not supported by the employed hardware, we always refer to active power.

In order to make the EV flexibility product a tradable asset, appropriate regulations and requirements should be introduced. Establishing standardized tests for evaluating the charger and EV performance are needed to categorize the supplied EV flexibility product. So, a deep knowledge of the controlled hardware performance is needed, including the EV charger efficiency for different set-points (presented in Section 3), to assess the accumulated losses during a V2G session. Such insights into the charger's efficiency can guarantee to the charger operator an accurate estimation of the real amount of energy flowing in/out of the battery. This is a necessary information for a safe and effective fleet operation, provided that low efficiencies may challenge the business case due to additional energy costs. Beside the necessity of a charging/discharging efficiency test, it is of utmost importance also to define the relevant charachteristics of the flexible EV when controlled for providing a power system service as FCR [3], to validate the fulfilment of the required performance. In this respect, we list seven attributes that have been experimentally assessed on V2G real hardware, the results of which are reported in Section 5:

(i) Direction: The information if an EV can provide only unidirectional or bidirectional (V2G) power flow.

(ii) Set-point linearity: The discreteness of the charging/discharging power set-point.

(iii) Starting time and maximum activation time: The period between receiving the set-point and activating the flexibility.

(iv-v) Ramp-up/ramp-down time: The up/downwards time between activation time and full service provision, and vice versa.

(vi) Accuracy: The difference between the required and the delivered response, e.g., the acceptable response band.

(vii) Precision: The variation of the delivered response for a given set-point.

Fig. 1 shows attributes *(iii)-(vii)* for an EV flexibility product, highlighting the difference between requested and provided power when controlling a flexible EV.

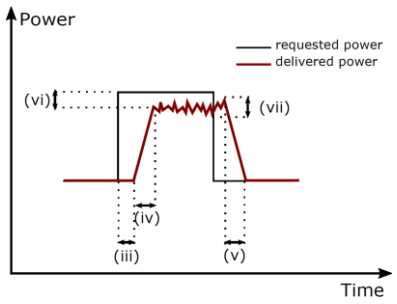

Fig. 1. Attributes *(iii)-(vii)* for an EV flexibility product.

3. LOCALLY AND REMOTELY CONTROLLED EVS PERFORMANCE TESTS

The first tests we present aim at assessing the efficiency of the V2G charger for a number of set-points. This is done in a local fashion, i.e., the set-points have been manually and locally set on the hardware, enabling us to derive the activation time of only the employed hardware. In order to evaluate the influence on the total activation time of additional communication latencies, the second tests were performed in a remote control fashion. The remote control test setup includes the communication and control infrastructure utilized by an actual EV aggregator, operating in on-field projects such as the Danish-funded projects ACES [5] and Parker [6]. Fig. 2 as a whole shows the test configuration for the centralized control architecture, enabling us to derive the total activation time including communication latencies. In this case the EVSE receives a power set-point remotely computed, and responds accordingly setting appropriate power flows in/out of the battery. With this design the aggregator calculates in a centralized way the appropriate V2G control signals to dispatch to its EVs, e.g., according to system frequency measurement in case of FCR. In case of the first local tests, the EV fleet operator platform is not utilized, whereas the set-points are directly set on the EVSE computer embedded in the charger.

In the proposed test activities two different active power test patterns were sent to the V2G-capable EVSE/EV. The first one is

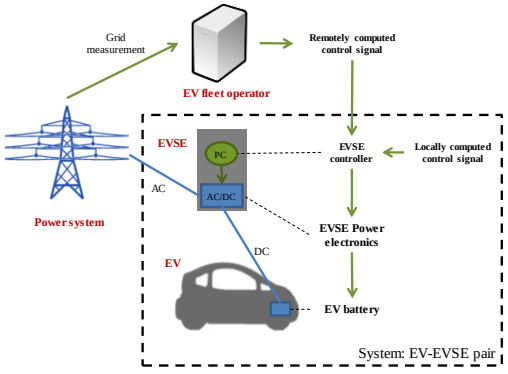

Fig. 2. Test configuration for the local and the remote control tests.

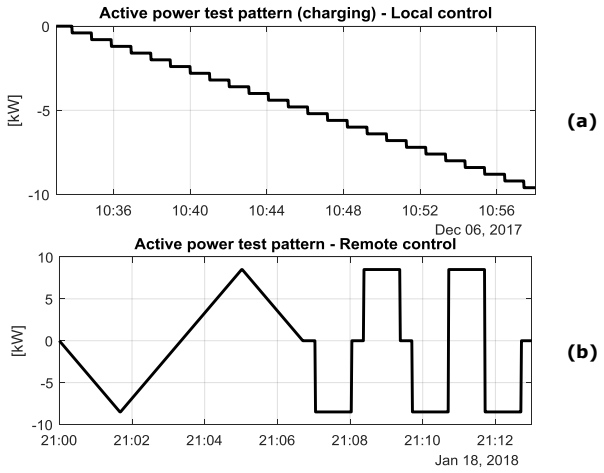

Fig. 3. Active power test patterns.

outlined in Fig. 3-a and represents different charging/discharging setpoints modulation from -10kW to +10kW with steps of 400 W. This test pattern allows the operational characterization of the V2G charger in terms of efficiency mapping. For the remote control test (Fig. 3-b), the pattern is designed in a way to allow an estimation of the seven flexibility service attributes defined in Section 2. Firstly, it enables us to validate the bidirectional capability and to assess total response time when controlling EVs in a remote fashion, including both communication latencies and charger and EV response time. This information is of utmost importance when assessing the capabilities on the provision of time-critical power system services from aggregated small distributed energy resources. Secondly, the remote test pattern consists first of a continuous and then of a step-wise variation of the charging/discharging power set-points. Such a cycle allows the measurement of the other five identified flexibility service attributes: the continuous part of the pattern allows the estimation of the step size granularity, whereas the step-wise part allows the estimation of the ramping times, the accuracy and the precision. Fig. 3-b shows the test cycle, which in practice was identically repeated 4 times, in order to have a more reliable measurement dataset for a more exhaustive and precise performance evaluation. Although the charger's size is ±10 kW, The extreme power set-points are ±8.5 kW due to an internal limitation set on the internal charger software

4. OUTCOME OF LOCAL CONTROL TESTS

The local control test intends to quantify the charger efficiency at all possible charging and discharging levels at different SOC. The tests where performed with a 30 kWh Nissan LEAF parked in a laboratory with 20°C for more than 24 hours. The AC side is measured with a DEIF MIC-2 power meter with 0.2 % accuracy and the DC side is measured with the internal DC voltage and current probe of the V2G charger, each with 1 s sample rate. The full range of the SOC is necessary to quantify the effect of changes in the internal battery voltage. This is achieved by repetively stepping through the possible charging/discharging setpoints with 1 A steps at the DC side, i.e., 400 W in case of 400 V DC – note that the actual DC power will depend on the DC voltage. For each power set-point, the efficiency is calculated and plotted in Fig. 4 with one line for each cycle, with the average SOC during the cycle, to assess the SOC influence on the efficiency. The discharge cycle is repeated until the Battery Management System (BMS), disconnects the EV as it reaches its internal discharge limit of 35%.

4.1. Calculation of efficiency map

In a first attempt we calculated the efficiency during a FCR provision session, and it resulted in a large variance of efficiency values for each power set point due to the large time constant of the charger, and the constantly changing set-point [11]. To avoid this problem, we decided to change the power setpoint only with one minute intervals, giving each charge/discharge cycle a 25 minute duration. The efficiency calculated for each DC power setpoint value is the average during the whole minute, giving a granularity of 25 values for each SOC level.

The results reported in Fig. 4 show that the large difference in the SOC has a negligible influence on the efficiency. The tests were performed only in the SOC range where the voltage changes linearly, so eventual difference in the results when operating in the extreme regions are not considered. However, it is not relevant considering the BMS limits in the useable range of the battery.

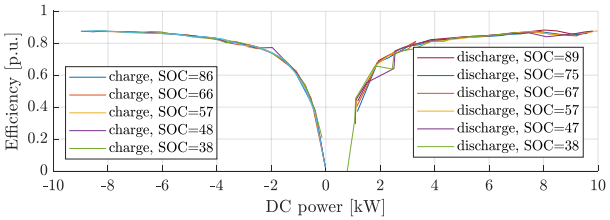

Fig. 4. V2G charger efficiency map for charging/discharging DC setpoints from -10kW to +10kW with steps of 400 W.

4.2. Calculation of activation time

The set-point control signal and the AC power provided on the grid side are shown in Fig. 5-a, which is a zoom-in of a part of the AC power measured during the charging test of Fig. 3-b. The time shift represents the activation time given the employed local control setup, thus it includes only the actual hardware response without any additional latencies due to control communications. Fig. 5-b shows the correlation of the two signals when applying different time shifts to one of them for the whole duration of the test. The maximum is found for a shift of 4 s, which is then considered as the activation time of the tested V2G equipment.

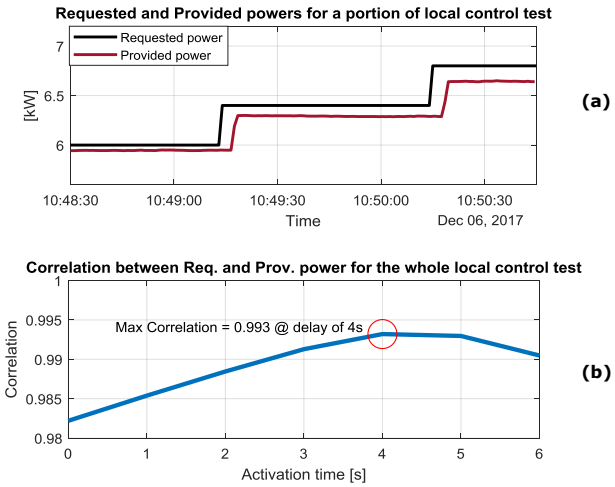

Fig. 5. The correlation between requested and provided power for local control shows a maximum for a delay of 4 s, which can then be considerd as the actual hardware response time.

5. OUTCOME OF REMOTE CONTROL TESTS

This Section presents the results of the performace test with the remote control setup. Note that the hardware under test and the laboratory environment conditions are the same as for the local control test.

Fig. 6 shows the required and the provided power of one cycle of the active power test pattern. In general, a time shift can be noticed, which here represents the total activation time given the employed remote control setup. Then, one can note the non-perfect linearity in the response to the signal in the continuous portion due to the set-point granularity imposed by protocols and the power electronics in the V2G charger. Finally, the time needed to reach the set-point is utilized for the calculation of the ramping rates, while the measured power at the stable set-point levels allows the calculation of accuracy and precision.

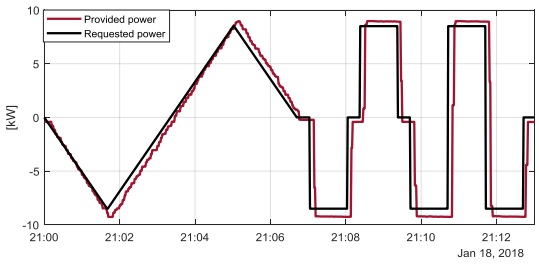

Fig. 6. 1 cycle of the performed remote performance assessment test.

5.1. Calculation of set-point linearity

The linearity in the response is studied in the continuous portion of the tested cycles, when a continuous linear setpoint is sent to the unit. The amplitude of the granular response is calculated as the difference of the measured provided power calculated at two consecutive time stamps. Hence a number of set-point granularities are calculated, which are then analysed.

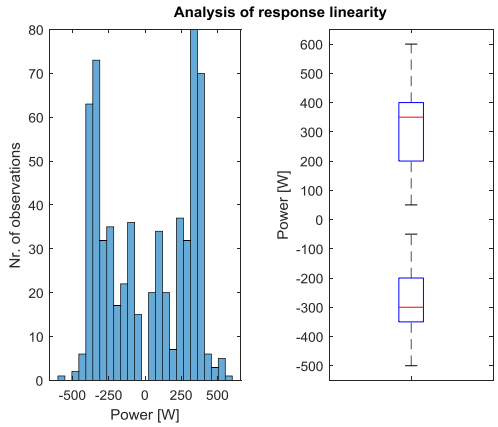

Fig. 7. Distribution of the observed granularities in terms of absolute and percentage observations. For the boxplots, the blue boxes indicate 50% of the observations, whereas the median is in red. Upper and lower quartiles (25% of the data) are located within the vertical black lines.

In this response linearity analysis we have excluded two sources of probable errors: the unavoidable noise in the measurements, and the response precision when setting a given set-point value. So, the calculation of the response linearity is done after applying a manual discreteness of 50 W on the measured data, given the average precision in the response calculated in subsection 5.4.

Results are reported in Fig. 7. The barplot shows the distribution of the observed granularities for different positive or negative sizes. First, the symmetrical distribution for charging (<0) and discharging (>0) can be noticed. Then the 2 bars with more observations (~50%) cover the range ±{300 400}W, whereas only in few cases (less than 5%) the absolute value of the granularity is > 400 W. The same results are reported in the boxplots, which show the median values -300 W and +350 W.

In general, one can conclude that in very few cases the EV responds with a discreteness larger than 400 W when controlled with a linear signal. 400 W in AC can thus be considered as the finest response granularity for the hardware under test. In this case, neglecting conversion losses, 400 W in DC means a granularity of 1 A, being the DC link voltage equal to 400 V, according to the technical CHAdeMO protocol.

5.2. Calculation of total activation time

The time shift shown in Fig. 6 represents the total activation time given the employed remote control setup, which includes both the 4 s delay of the actual hardware response time found in Section 4, and the additional latencies due to the centralized control architecture. Fig. 8 shows the correlation of the two signals of Fig. 6 when applying different time shifts to one of them. The maximum is found for a shift of 7 s, which is then considered as the total activation time when the tested V2G equipment is controlled via the centralized remote control setup.

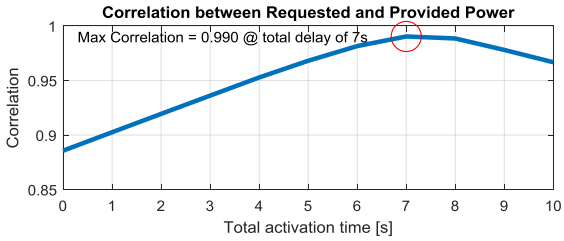

Fig. 8. The correlation between requested and provided power for remote control shows a maximum for a delay of 7 s, which can then be considerd the total activation time when the tested V2G equipment is controlled via the centralized remote control setup.

By comparing this analysis with the similar one proposed in Section 4 for local control, an assessment of the influence on the overall response time only due to a centralized control architecture can be derived. This validation can then provide a valuable information on the actual total activation time capabilities given either a local or a remote control. Such information is of utmost importance when assessing the capabilities on the provision of time-critical power system services from aggregated small distributed energy resources, so when evaluating whether to implement a centralized or a decentralized control strategy.

5.3. Calculation of ramping up/down

The ramping up/down capabilities are studied in the step-wise portion of the tested cycles, where 4 events up and 4 events down are performed as shown in Fig. 9. The charging power is changed from the zero set-point to the minimum and maximum values, back to zero. Also the largest possible steps are analysed, i.e., when setting the maximum power starting from the minimum set-point, and vice versa.

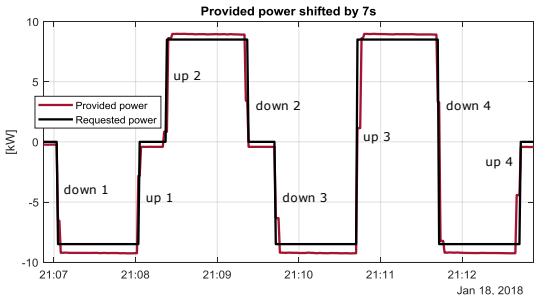

Fig. 9. For each cycle of the performed performance assessment test 4 events up and 4 events down are performed to calculate the ramping rate capability. For the step-wise portion, 4 cycles have been repeated.

Table 1 Measured ramping rates up/down.

	Cycle 1	Cycle 2	Cycle 3	Cycle 4
up 1	8.84kW in 3s	8.84kW in 4s	8.82kW in 3s	8.84kW in 4s
up 2	9.03kW in 4s	9.04kW in 4s	9.03kW in 4s	9.04kW in 5s
up 3	17.87kW in 6s	17.85kW in 6s	17.88kW in 4s	17.86kW in 6s
up 4	8.84kW in 4s	8.84kW in 1s	8.83kW in 4s	8.84kW in 3s
Ramp-up AVG	**3.35 kW/s**			
down 1	8.99kW in 3s	8.79kW in 4s	8.79kW in 4s	8.99kW in 3s
down 2	9.33kW in 3s	9.16kW in 1s	9.17kW in 1s	9.16kW in 4s
down 3	8.79kW in 4s	8.98kW in 3s	8.97kW in 4s	8.99kW in 4s
down 4	18.12kW in 6s	18.14kW in 7s	18.13kW in 7s	18.14kW in7s
Ramp-down AVG	**3.31 kW/s**			

Table 1 reports numerical results of the calculated up/down ramping rates. The average up and down rates almost coincide, and are equal to about 3.3 kW/s when expressed in the general unit of measurement [kW/s], i.e., related to 1 s time window. Nevertheless, the minimum calculated up and down rates are 1.8 kW/s (up2-cycle4) and 2.2 kW/s (down1-cycle2,3 and down3-cycle1) respectively, which is way lower than the average. This means that the unit on averege responds with 3.3 kW/s, but may respond slower.

This outcome is very important, as it can be valuable information for grid operators when performing grid regulation studies, assessing the impacts of grid regulation services provided by such units. Moreover, it can be useful also when defining requirements for grid connected V2G technologies, provided the knowledge of the technology under exam.

5.4. Calculation of set-point accuracy

The calculation of the set-point accuracy is done during the constant set-point levels of the step-wise portion of the tested cycles, as highlighted in Fig. 10. The accuracy is calculated as the difference between the requested and the provided power over the appropriate time windows.

It was found that for charging operations (power<0) the power drawn from the grid is larger than the requested power. The same happens in case of zero set-point, where the power consumption is justified as the own consumption of the power electronics on stand-by mode. During the discharge operations, the power injected into the AC grid is higher than expected. This is probably due to a wrong calibration of the internal EV charger power electronics, which should be tuned to avoid higher injection of power higher than the requested value, as it could compromise the safe operation.

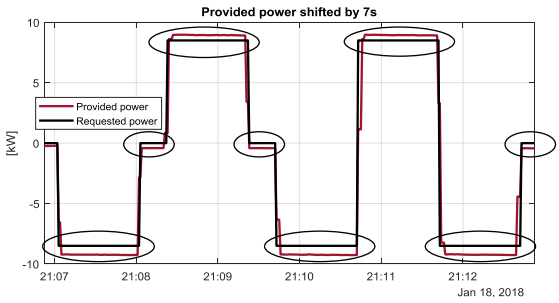

Fig. 10. For both accuracy and precision the calculation is done during the constant set-point levels of the step-wise portion of the tested cycles. This means at zero set-point at the maximum charging (-8.5 kW) and discharging power (+8.5 kW).

At zero set-point the charger drawns from the grid on average 420 W, which can then be considered as the unit's stand-by loss. In case of full charging operation (requested power = 8.5 kW), the calculated accuracy is 740 W, which represents the 8.7% of the power set-point. Such accuracy is higher than the stand-by losses, probably due to a non-optimal calibration of the unit. Finally, during the full discharging operation (requested power = -8.5 kW) an unexpected power value higher than the requested one was measured. Results show that the average power provided is higher than the requested by 440W, which is the 5.2% of the power set-point.

5.5. Calculation of set-point precision

As done for the accuracy, the precision is calculated during the constant set-point levels of the step-wise portion of the test cycles. The accuracy is calculated as the difference between the maximum and the minimum values of the provided power over the whole length of the time windows with stable extreme set-points. This means that the precision calculated with this test cycle can be considered as the worst case as for the extreme charging and discharging set-points.

It is found that the precision is about 50 W for both the extreme charging and discharging operation. This value justifies the choice of 50 W as manual discretization factor that has been utilized in the analysis of the granularity presented in subsection 5.1. In case of zero-setpoint the precision was much higher, since the difference between maximum and minimum of the measured power was about 6 W.

5. DISCUSSION AND CONCLUSIONS

In this paper the technical capabilities of a commercial V2G CHAdeMO charger have been identified to assess the suitability of such technology for grid service provision. Specifically, the importance of the knowledge of the efficiency for all the possible operating conditions has been highlighted, along with the seven attributes of a flexibility product to be traded in the market. Moreover, two different test setups were utilized to investigate how the total activation time would change in case of local or remote control. This provided crucially valuable information when assessing the capabilities on the provision of time-critical power system services from aggregated small distributed energy resources.

Table 2 shows the summary outcome of the performance tests results for each identified flexibility product attribute, with the respective performance target defined by current technical standards. In particular, the requirements have been adapted from the Danish technical standard for FCR provision [3] and the newly released Danish technical regulation for grid connected battery plants, which applies also for a number of aggregated EV chargers providing V2G services [12]. Such requirements are then considered as benchmarks when evaluating the eligibility of EVs in FCR service provision.

Table 2 Evaluation test results.

Attribute	**Short description**	**Unit**	**Target for Primary Reserve [3], [10]**	**Test result**
(i) Direction	Support of bidirectional power flow	+/-/±	±	± i.e. V2G capable
(ii) Set-point linearity	Supported setpoint throughout the power range	[W]	Linear at 1%	< 400 W (4%) (1 A @ 400V DC)
(iii) Starting time and maximum activation time	Time between setpoint request and change in active power	[s]	< 15 s	Local control: 4 s Remote control: 7 s
(iv) Ramp-up time	Supported rate of change in power (increase)	[kW/s]	For the aggregate: 10-300 kW/s	AVG = 3.35 kW/s Max = 8.84 kW/s min = 1.81 kW/s
(v) Ramp-down time	Supported rate of change in power (decrease)	[kW/s]	For the aggregate: 10-300 kW/s	AVG = 3.31 kW/s Max = 9.17 kW/s min = 1.98 kW/s
(vi) Accuracy	Difference between required and delivered response	[W]	±5% of setpoint & ±0.5% of rated pow.	Negative setpoint: 740W (+8.7% of setpoint) (+7.4% of rated pow.) Positive setpoint: -440W (-5.2% of setpoint) (-4.4% of rated pow.) 420 W @ zero setpoint (4.2% of rated pow.)
(vii) Precision	Variation of the delivered response	[W]	±5% of setpoint & ±0.5% of rated pow.	≈ 50 W (0.6% of setpoint) (0.5% of rated pow.) 6 W @ zero setpoint (0.06% of rated pow.)

Going through the seven attributes, firstly it can be seen that the symmetric power reserve bid requested by [3] applies to a bidirectional power flow capability, which is available due to the V2G technology. As for the set-point linearity, generally a linearity of 1% of the rated power is requested. It is found that the finest response has a granularity of 400 W, which represents the 4% of the rated power, thus not fulfilling the requirement. However, as this is the linearity for only one single unit, when managing an EV fleet the fleet operator should then apply smart logics, e.g., based on stochastic logics aimed at reaching – as proposed in [13] – the required target on an aggregated level. As for the activation time, the latencies due to remote control communication amount to about 3 s, while the mere hardware is

characterized by an activation time of 4 s. Ref. [3] requires the activation of half of the full capacity within 15 s, which is then respected considering an instantaneous response. In reality, the response has an up-down ramping rate, which amounts to an average value of 3.3 kW/s. For the tested charger, this means that the total activation time for half of the reserve (5 kW) would be about 8.6 s, which is lower than the requested 15 s. Ref. [12] requires a ramping rate capability for the aggregated fleet within the range of 10-300 kW/s, which is out of the range of capabilities of the single units. This means that, considering again the everage value of 3.3 kW/s, the minimum and maximum number of EVs to be employed for matching the required 10-300 kW/s ramping range will be 3 and 91, respectively. Finally for accuracy and precision, [12] requires a response within ±5% of the set-point and ±0.5% of the rated power. The requirement on the precision is respected, wheres for the accuracy, the limits at the two maximum charging and discharging levels are overcome. This issue may be dealt with proper calibration of the internal power electronics that should be tuned to avoid such inaccurancies. Furthermore, as the requirements refer to the overall battery plant, smart fleet management solutions could be implemented, to reduce the reserve provision error via appropriate individual control of the single EVs, e.g., as proposed in [13].

To conclude, in order to make the EV flexibility product a tradable asset, relevant regulations and requirements should be respected, and standardized tests for evaluating charger's and EV's performance should be established. In fact, a deep knowledge of the controllable hardware is needed to categorize the supplied EV flexibility product. On the one hand, insights into the charger's efficiency for different set-points allow the calculation of the accumulated losses during a V2G session, which is a crucial information for the estimation of the actual state of charge of the controlled EV. On the other hand, the proposed investigation of the identified charachteristics of the V2G unit provides valuable information for grid operators when performing grid regulation studies, assessing the impacts of FCR provided by such units with realistic models to emulate their behavior. Furthermore, it can be useful also when defining new requirements for grid connected V2G technologies, provided an orientative knowledge of the employed technology's capabilities. Ultimately, the proposed investigation results provide insights also for the EV fleet operators in terms of actions needed for smart fleet management aimed at respecting the grid code restrictions.

ACKNOWLEDGMENTS

The authors would like to acknowledge the support of the EUDP project ACES - Across Continent Electric Vehicle Services (grant EUDP17-I-12499, website: www.aces-bornholm.eu) and the Danish research Parker project under ForskEL contract no. 2016-1-12410, http://parker-project.com.

REFERENCES

[1] M. N. B. Arias, S. Hashemi, P. B. Andersen, C. Træholt, and R. Romero, "V2G Enabled EVs Providing Frequency Containment Reserves: Field Results," in *2018 IEEE International Conference on Industrial Technology (ICIT 2018)*, 2018, pp. 1–6.

[2] K. Knezović, S. Martinenas, P. B. Andersen, A. Zecchino, and M. Marinelli, "Enhancing the Role of Electric Vehicles in the Power Grid : Field Validation of Multiple Ancillary Services," *IEEE Transactions on Transportation Electrification*, vol. 3, no. 1, pp. 201–209, 2016.

[3] Energinet.dk, "Danish Technical Standard: ancillary services to be delivered in Denmark - tender conditions," *https://en.energinet.dk/-/media/Energinet/El-RGD/Dokumenter/Ancillary-services-to-be-delivered-in-Denmark.pdf*, 2017. .

[4] A. Thingvad, S. Martinenas, P. B. Andersen, M. Marinelli, C. Bjørn E, and O. J. Olesen, "Economic Comparison of Electric Vehicles Performing Unidirectional and Bidirectional Frequency Control in Denmark with Practical Validation," in *2016 Proceedings of the 51st International Universities Power Engineering Conference*, 2016, pp. 1–6.

[5] "ACES project - across continents electric vehicle services," *http://aces-bornholm.eu*, 2017. .

[6] "The Parker project," *http://parker-project.com*, 2016. .

[7] "INVENT project - Intelligent Electric Vehicle Integration," *https://rmp.ucsd.edu/_files/sei/INVENT-Flyer.pdf*, 2017. .

[8] "GridMotion project - reducing electric vehicle usage cost thanks to smartcharging process," *https://www.enel.com/content/dam/enel-common/press/en/1667129-2_PDF-1.pdf*, 2017. .

[9] NISSAN, "Nissan, enel and nuvve operate world's first fully commercial vehicle-to-grid hub in denmark," *http://www.nissan-helsingor.dk/index.php/om-os/nyheder/show/news/id/4*, 2016. .

[10] K. Knezović, M. Marinelli, A. Zecchino, P. B. Andersen, and C. Træholt, "Supporting involvement of electric vehicles in distribution grids: Lowering the barriers for a proactive integration," *Energy*, 2017.

[11] A. Thingvad, C. Ziras, J. Hu, and M. Marinelli, "Assessing the Energy Content of System Frequency and Electric Vehicle Charging Efficiency for Ancillary Service Provision," in *Proceedings of the 52nd International Universities' Power Engineering Conference*, 2017, pp. 1–6.

[12] "Danish Technical regulation 3.3.1 for battery plants." 2017.

[13] C. Ziras, A. Zecchino, and M. Marinelli, "Response Accuracy and Tracking Errors with Decentralized Control of Commercial V2G Chargers," in *20th Power Systems Computation Conference (PSCC 2018)*, 2018, pp. 1–7.